

Optical Pumping of Rubidium

Brandon Ling, Daniel Smith, AdLab, Boston University, Boston MA 02215

We use optical pumping to measure the Landé g-factors of ^{87}Rb and ^{85}Rb . We find $g_{87} = 0.51 \pm 0.02$ and $g_{85} = 0.34 \pm 0.01$. We also observe the splittings due to the linear and quadratic Zeeman effects, and calibrate the Helmholtz coils for use by future groups on this experiment.

INTRODUCTION

Optical pumping is a common technique used in constructing lasers. Light is used to excite (or pump) electrons in an atom from a lower energy level to a specific higher level. Alkali metals are often used because they have only one valence electron, so that the electron can be treated like in hydrogen. In the case of rubidium, external DC and RF magnetic fields are used to manipulate the population of the excited state.

We must take into account the interaction between the electron and the nucleus as well as between the electron and the magnetic field. The following discussion is adapted from [1]. The main contribution to the Hamiltonian of the system is the familiar Coulomb interaction H_C :

$$H_C = \frac{\mathbf{p}^2}{2m} - \frac{Ze^2}{r}. \quad (1)$$

On top of this there are several splittings. The first is due to the spin-orbit coupling, which arises from the interaction between the spin magnetic moment and the magnetic moment of the electron's orbit. These levels are known as the fine structure, and the typical splitting is of the order 10^{-4} eV.

Next is the splitting from the interaction of the magnetic moment of the electron with the nuclear magnetic moment, known as the hyperfine splitting. The typical splitting is of order 10^{-6} eV.

The final splitting is due to the presence of the external magnetic field. This effect is known as the Zeeman effect. The classical magnetic moment μ of a particle with charge q is $\mu = q/2m\mathbf{L}$ where \mathbf{L} is the orbital angular momentum. Quantum mechanically we have

$$\mu_J = -g_J \frac{e}{2m} \mathbf{J} \quad (2)$$

$$\mu_F = -g_F \frac{e}{2m} \mathbf{F} \quad (3)$$

where μ_J is the magnetic moment from the total electronic angular momentum \mathbf{J} , and μ_F is the total magnetic moment of the atom due to the total atomic angular momentum \mathbf{F} . The factors g_J and g_F are known as the Landé g-factors which provide the quantum correction to the magnetic moments. For a small magnetic field of magnitude B_z along

the z-direction, the energies are proportional to the applied field:

$$H_B = g_F \mu_B m_F B_z \quad (4)$$

where μ_B is the Bohr magneton, and $m_F \hbar$ is the eigenvalue of the operator F_z .

For larger fields, we must diagonalize the following Hamiltonian:

$$H = H_{\text{hf}} + H_B = A \mathbf{J} \cdot \mathbf{I} + g_J \mu_B \mathbf{J} \cdot \mathbf{B} \quad (5)$$

where A is some constant and \mathbf{I} is the nuclear spin. The result of diagonalizing is known as the Breit-Rabi formula:

$$\frac{\Delta E(F_{\pm}, m_F)}{\Delta E_{\text{hf}}} = -\frac{1}{2(2I+1)} \pm \frac{1}{2} \sqrt{1 + \frac{4m_F}{2I+1} x + x^2} \quad (6)$$

where $F_{\pm} = I \pm \frac{1}{2}$, and the dimensionless parameter

$$x \equiv \frac{g_J \mu_B B}{\Delta E_{\text{hf}}} \quad (7)$$

and ΔE_{hf} is the hyperfine splitting with no magnetic field. Fig.1 shows a diagram of the splittings of the energy levels. Fig.2 shows plots of the Breit-Rabi equation.

We are interested in using optical pumping to measure the Landé g-factors g_F of the two naturally occurring isotopes of rubidium, ^{85}Rb and ^{87}Rb . We describe optical pumping in more detail in the following section.

EXPERIMENTAL SETUP

Light from a Rb lamp consisting mainly of two main lines, one at 780 nm and one at 795 nm is sent through an interference filter, eliminating the 780 nm line since we are interested in transitions from the $^2S_{1/2}$ states to the P states. The light then passes through a linear polarizer and then a quarter wave plate to produce circularly polarized light. The light is then sent through the Rb vapor cell and the intensity is monitored by a photodiode detector. A DC magnetic field is applied along the

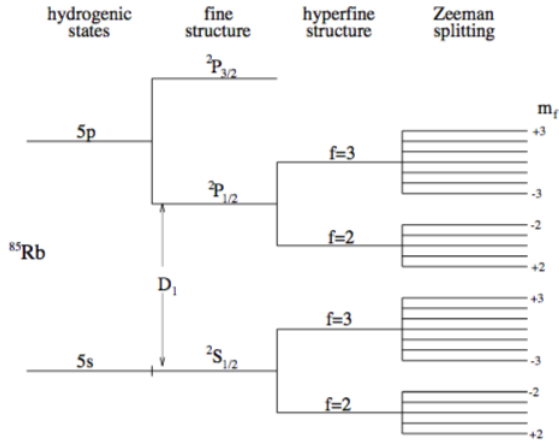


FIG. 1: The energy levels of the valence electron of ^{85}Rb . We see how each correction splits the energies.

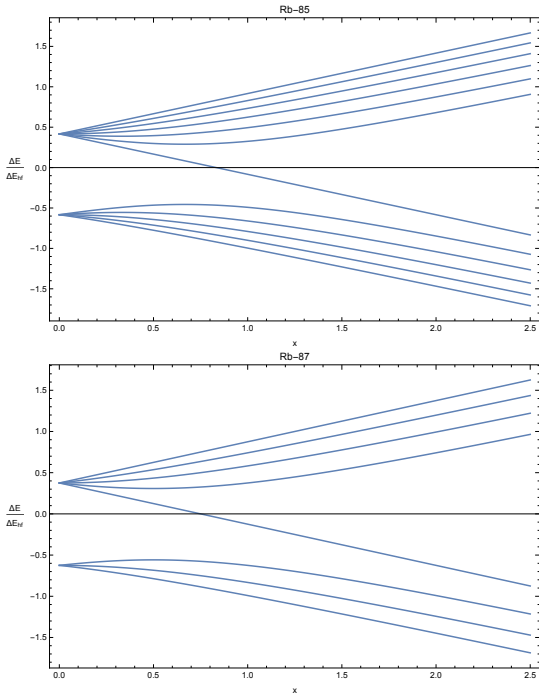


FIG. 2: The Breit-Rabi equation (in dimensionless form) showing the energy splittings. We can see the low and high field regimes are linear.

optical axis horizontally, as well as vertically by a set of Helmholtz coils. A transverse RF magnetic field induces transitions. A pair of smaller horizontal coils, known as the sweep coils, are also applied along the optical axis. These are used to fine-tune the applied horizontal magnetic field. The controller for the coils allows the current, and hence the magnetic

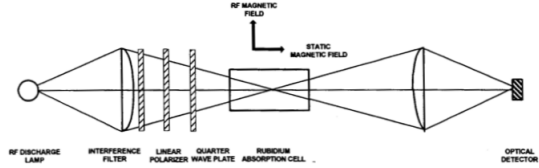


FIG. 3: a schematic of the apparatus. Figure taken from [2].

field, to be ramped up. See Fig. 3.

Due to conservation of angular momentum, only transitions involving $\Delta m_F = +1$ (or -1 depending on whether the light is left- or right-circularly polarized) are allowed. For the purposes of this discussion, we take the polarization to be such that $\Delta m_F = +1$. Transitions occur within the Zeeman levels, as well as between the S and P states. When an excited state spontaneously decays, the resulting photon is not restricted by the above selection rule, so that the excited state may decay into essentially any lower energy state. However, the highest m_F state of the $^2S_{1/2}$ states cannot be excited to any of the $^2P_{1/2}$ states since there is no available state with $m_F + 1$. For ^{85}Rb , this corresponds to the $^2S_{1/2}, f = 3, m_F = +3$ state. See Fig. 1. Note there is no state with $m_F = +4$. Thus the result is that this level will have an increase in population, so that the distribution of the energy levels will be different from the Boltzmann distribution. Since the atoms in this level cannot absorb the photons, the transmitted intensity will become larger.

We use the RF coils to create transitions with $\Delta m_F = \pm 1$, and use the photodiode to record the transmitted intensity. In order to measure the g-factors, we use the low-field regime, Eqn. 4, to obtain the transition frequencies ν :

$$\nu = g_F \frac{\mu_B}{h} B. \quad (8)$$

RESULTS AND ANALYSIS

We first observed the zero-field transition, which corresponds to the 5S to 5P transitions. Then, setting the RF field to 150 kHz (i.e. the desired transition frequency), we used the sweep coils to ramp up the magnetic field to observe the separate absorption lines of ^{85}Rb and ^{87}Rb . An example trace from the oscilloscope is shown in Fig. 4 We use the geometry of the Helmholtz sweep coils to determine the magnetic field of the coils as a function of current. The mean radius is 0.1639 m, and there are 11 turns in each coil. As given in [2], the magnetic field (in

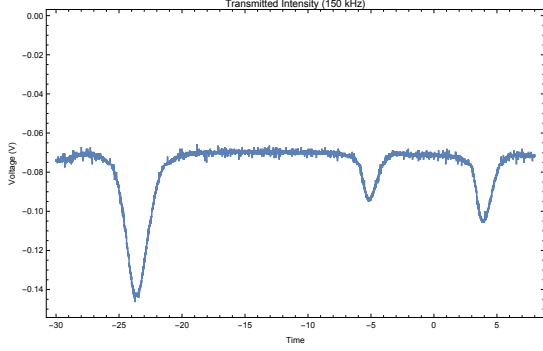


FIG. 4: The absorption lines at low magnetic field, with resonant frequency equal to 150 kHz. The leftmost dip is the zero field resonance. The middle is from ^{87}Rb , and the rightmost is from ^{85}Rb .

gauss) is then given by

$$B = 8.991 \cdot 10^{-3} \frac{11}{0.1639 \text{ m}} I. \quad (9)$$

We measured the sweep currents at which there is resonance for several different RF transition frequencies and converted them to magnetic field values. Then, using Eqn. 8, we compute the g-factors. We obtain the following weighted averages:

$$g_{87} = 0.52 \pm 0.03$$

$$g_{85} = 0.344 \pm 0.014.$$

The accepted values are $g_{87} = 1/2$ and $g_{85} = 1/3$ [2]. Our results differ by 4% and 3%, respectively.

Using the accepted values for the g-factors, we then calibrated the sweep coils as well as the main coils more accurately for future use. To calibrate the sweep coil, we used the resonance equation 8 to compute the magnetic field for each RF transition frequency. Then we computed a linear fit to the sweep coil magnetic field vs sweep coil current. We found

$$B_{\text{sweep}} = (0.618 \pm 0.014 \frac{\text{gauss}}{\text{A}}) I - (0.128 \pm 0.010) \text{ gauss} \quad (10)$$

See Fig. 5. The χ^2 value for this fit is

$$\chi^2 = 9.18 \quad \text{for } 8 \pm 4 \text{ degrees of freedom.} \quad (11)$$

To calibrate the main coils, we calculated the total magnetic field using the resonance equation:

$$B_{\text{tot}} = \frac{h \nu}{\mu_B g_F}. \quad (12)$$

Using our equation above for B_{sweep} , we calculate B_{main} by $B_{\text{main}} = B_{\text{tot}} - B_{\text{sweep}}$. We find

$$B_{\text{main}} = (8.633 \pm 0.004 \frac{\text{gauss}}{\text{A}}) I \quad \text{gauss.} \quad (13)$$

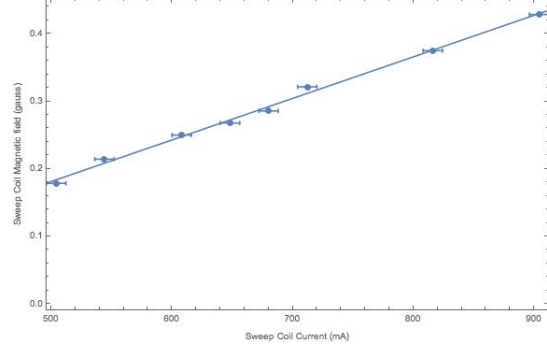


FIG. 5: A plot of the sweep coil magnetic field vs sweep coil current. Note the vertical error bars are smaller than the point size.

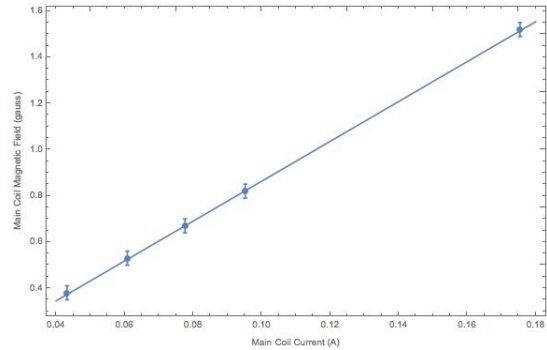


FIG. 6: A plot of the main coil magnetic field vs coil current. Note the horizontal error bars are smaller than the point size.

See Fig. 6. The χ^2 value for this fit is

$$\chi^2 = 0.135 \quad \text{for } 5 \pm 3 \text{ degrees of freedom.} \quad (14)$$

At the very end of the experiment we were able to move into the intermediate magnetic field regime and observe the so-called quadratic Zeeman splitting [2] for ^{85}Rb . See Fig. 7. Theory predicts 10 absorption lines, but we were only able to observe 9. We are not sure why we do not see all 10. A future group working on this experiment should investigate why, and could also measure the transition energies and compare them to the Breit-Rabi equation 6.

We checked for possible systematic errors. The first thing we did was retune the vertical magnetic field of the vertical Helmholtz coils. The current through them had been kept at 1.35 mA. We retuned the field by looking at the zero-field resonance and varying the vertical field strength to minimize the linewidth. We set the current to 1.36 mA, but there was no significant difference.

We used the same procedure to fine-tune the horizontal alignment of the table. The optical axis is supposed to be aligned along the local north-south

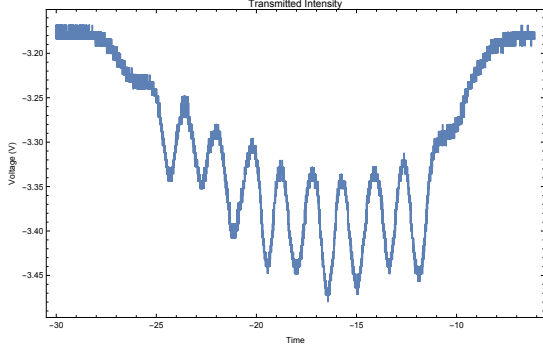


FIG. 7: The absorption lines for ^{85}Rb in the intermediate magnetic field regime. The RF transition frequency was 3.62 MHz. There are only 9 absorption lines, whereas theory predicts 10.

magnetic field line. There is a fine-tune knob on the table to rotate the table, and we ended up turning it a quarter-turn clockwise compared to the original configuration. With this, we redid the experiment, obtaining the following results:

$$g_{87} = 0.50 \pm 0.03 \quad (15)$$

$$g_{85} = 0.335 \pm 0.015 \quad (16)$$

Combining this with our previous measurements, our best estimate for the g-factors are

$$g_{87} = 0.51 \pm 0.02 \quad (17)$$

$$g_{85} = 0.34 \pm 0.01. \quad (18)$$

The fractional uncertainties are 4% and 3%, respectively.

CONCLUSIONS

We measured the Landé g-factors of ^{87}Rb and ^{85}Rb to be 0.51 ± 0.02 and 0.34 ± 0.01 , respectively. We were also able to qualitatively observe the linear Zeeman splittings, and the quadratic Zeeman splittings for ^{85}Rb , although we were unable to observe all of the predicted quadratic splittings.

ACKNOWLEDGEMENTS

I would like to thank my lab partner Daniel for all of his help and insights. I would also like to thank Professor Sulak and Situ for their advice and assistance.

-
- [1] J. H. Taylor, S. Smith, B. Austin, and M. Romalis, “Optical pumping of rubidium vapor,” (2009).
 - [2] Teachspin, “Optical pumping of rubidium guide to the experiment,” (2002).